



# Method of movable lattice particles

V.L. Popov<sup>a,\*</sup>, A.E. Filippov<sup>b</sup>

<sup>a</sup>Technische Universität Berlin, Germany

<sup>b</sup>Donetsk Institute for Physics and Engineering of NASU, 83144 Donetsk, Ukraine

## Abstract

A new simulation technique for modeling elastoplastic deformation and friction processes based on the dynamics of a system of “lattice particles” is proposed. In usual simulation methods like molecular dynamics, only interactions compatible to the symmetries of space (invariant with respect to translations and rotations) are used. In the proposed method, the interaction potentials depend both on the relative position of particles and the orientation of their relative radius vector with respect to prescribed “lattice directions”. We show that in spite of this relation with the “external space”, the system behaves, in linear approximation, as an isotropic elastic medium invariant to both the translations and rotations of the medium as a whole. The coupling with the external space occurs to be a surface effect, which either does not play an important role (if the motions of the boundaries are prescribed) or can be handled properly by introducing fictive compensating surface forces. Introduction of forces depending on the orientation of the local surroundings of a particle makes it possible to describe elastic media with arbitrary elastic properties by using only interactions between the next neighbours. The system of lattice particles shows better stability properties and allows one to describe large plastic deformations, avoiding problems of “packaging” typical for many particle methods.

© 2006 Elsevier Ltd. All rights reserved.

Keywords: ■; ■; ■

## 1. Introduction

Numerical methods based on continuum models (finite elements) are very efficient in simulating various mechanical systems. However, a number of physical processes can be simulated within the framework of continuum approaches to only a very limited extent. These are primarily the processes whereby the medium continuity is impaired, i.e., those of nucleation and accumulation of damages and cracks, and failure of materials. One of the reasons for widespread continuum methods is that differential equations of continuum mechanics allowed using effective analytical methods developed during the last two centuries. The recent advancement in computer engineering has made this advantage of continuum models less significant. Having no negation of the importance of analytical methods, we should nevertheless state that an ever-increasing number of problems in mechanics are solved by “direct” computations. To this end, the successfully

continuum nature should be again discretized (e.g., in the finite element method). The reasons mentioned allow us to predict that in the immediate future, there will be a fast development of simulation methods based directly on the discrete representation of materials with no continuization of the latter as an intermediate step. We refer to these “directly discrete” methods as *particle methods*.

One of the first attempts of such a kind was made by Greenspan, who has used the Lennard–Jones interaction potentials in macroscopic many-particles systems [1]. A further step in developing the particle methods was the introduction of internal variables and of the “interaction” between the mechanical and the thermodynamic degrees of freedom in Refs. [2,3]. On this way, the thermal conductivity has been introduced in the discrete systems as well as dependence of interaction potentials on the stored thermal energy. As an example of a successful development of particle method for quantitative description of real media, we mention the method of movable cellular automata [4,5].

\*Corresponding author. Fax: +49 30 314 72575.

E-mail address: [v.popov@tu-berlin.de](mailto:v.popov@tu-berlin.de) (V.L. Popov).

1 How could the macro and meso approaches in the  
 3 method of particles be attempted? The first examples of its  
 5 applications have already shown that the particles method  
 7 has some specific difficulties. One of the most known is that  
 9 the properties of the particles system do strongly depend on  
 11 their “packaging”. Further, by using only the two-particle  
 potential, it is not possible to fit two elastic constants of an  
 isotropic elastic continua [6]. One of the solutions of this  
 problem is to use many-particle potentials either in the  
 form proposed in Ref. [7] or as it is made in the method of  
 movable cellular automata [6].

In the present paper, we propose a third way to describe  
 arbitrary elastic or plastic continua with particle methods.  
 We use a system of particles, ordered initially into a  
 hexagonal lattice, which do not “forget” this initial order.  
 For this purpose, we use interactions explicitly depending  
 on the underlying hexagonal symmetry of the model. We  
 show, however, that in spite of the underlying hexagonal  
 symmetry, the system behaves as an isotropic elastic  
 continuum with continuous rotation symmetry (in the  
 linear range). The situation is very similar to that with  
 lattice gases. Frisch et al. [8] have shown in 1986 that it is  
 possible to describe hydrodynamics of an isotropic liquid  
 with a “lattice gas”. They gave an example of a system of  
 binary elements on a hexagonal lattice with simple discrete  
 rules for a transition between states, which provides an  
 equation of isotropic incompressible viscous fluid in the  
 macroscopic limit. In the present paper, we show that a  
 similar approach is possible for describing elastic and  
 plastic properties of solids.

## 2. Linear elastic model

Consider a hexagonal lattice of mass points. We would  
 like to define the interactions between them in such a way,  
 that the system behaves macroscopically as an isotropic  
 elastic body. Let us define the lattice vectors as unit vectors  
 between the next neighbours in the not-deformed lattice:

$$e_i^\alpha = \left( \cos \frac{\pi}{3} \alpha, \sin \frac{\pi}{3} \alpha \right), \quad \alpha = 0, 1, 2, 3, 4, 5. \quad (1)$$

The index  $i$  stands for the Cartesian components  $x$  or  $y$ ,  
 and  $\alpha$  counts the next numbers (6 in a hexagonal lattice).  
 The length of a vector connecting two neighbouring centres  
 is denoted as  $c$ . If the mass points are moved from their  
 initial position in the lattice by  $u_i^\alpha$ , an interaction force  
 appears. The most general form of the linear interaction  
 between two neighbours in the direction of  $e_i^\alpha$  is

$$F_i^{0\alpha} = k_1(u_i^\alpha - u_i^0) + k_2 e_j^\alpha (u_j^\alpha - u_j^0) e_i^\alpha. \quad (2)$$

$F_i^{0\alpha}$  is the force acting on the centre zero from the centre  $\alpha$ .  
 Let us now suppose some smooth deformation field  $u(x)$   
 in the body. The force acting on the centre zero is then  
 equal to

$$\begin{aligned} F_i^0 &= \sum_{\alpha=0}^5 F_i^{0\alpha} = \sum_{\alpha=0}^5 k_1(u_i^\alpha - u_i^0) + k_2 e_j^\alpha (u_j^\alpha - u_j^0) e_i^\alpha \\ &= \sum_{\alpha=0}^5 (k_1(u_i(c\bar{e}^\alpha) - u_i(0)) \\ &\quad + k_2 e_j^\alpha (u_j(c\bar{e}^\alpha) - u_j(0)) e_i^\alpha. \end{aligned} \quad (3)$$

Expanding the field  $u_i$  up to the terms of second order, we  
 get

$$u_i(c\bar{e}^\alpha) - u_i(0) = c \frac{\partial u_i}{\partial x_j} e_j^\alpha + \frac{c^2}{2} \frac{\partial^2 u_i}{\partial x_j \partial x_k} e_j^\alpha e_k^\alpha. \quad (4)$$

Substitution into Eq. (3) gives

$$F_i^0 = \sum_{\alpha=0}^5 \left( k_1 \frac{c^2}{2} \frac{\partial^2 u_i}{\partial x_j \partial x_k} e_j^\alpha e_k^\alpha + k_2 \frac{c^2}{2} \frac{\partial^2 u_j}{\partial x_m \partial x_k} e_m^\alpha e_k^\alpha e_i^\alpha \right). \quad (5)$$

It is easy to show that

$$\begin{aligned} \sum_{\alpha=0}^5 e_j^\alpha e_k^\alpha &= 3\delta_{jk}, \\ \sum_{\alpha=0}^5 e_m^\alpha e_k^\alpha e_i^\alpha e_j^\alpha &= \frac{3}{4} (\delta_{mk}\delta_{ij} + \delta_{mi}\delta_{kj} + \delta_{mj}\delta_{ki}). \end{aligned} \quad (6)$$

The force (5) can thus be represented in the form

$$\begin{aligned} F_i &= \frac{3}{2} k_1 c^2 \frac{\partial^2 u_i}{\partial x_k^2} + \frac{3}{8} k_2 c^2 \left( \frac{\partial^2 u_i}{\partial x_k^2} + 2 \frac{\partial^2 u_k}{\partial x_i \partial x_k} \right) \\ &= \frac{3}{2} c^2 \left( k_1 + \frac{1}{4} k_2 \right) \frac{\partial^2 u_i}{\partial x_k^2} + \frac{3}{4} c^2 k_2 \frac{\partial^2 u_k}{\partial x_i \partial x_k} \end{aligned} \quad (7)$$

or in the vector form

$$\mathbf{F} = \frac{3}{2} c^2 \left( k_1 + \frac{1}{4} k_2 \right) \Delta \mathbf{u} + \frac{3}{4} c^2 k_2 \nabla \operatorname{div} \mathbf{u}. \quad (8)$$

Note that it is invariant with respect to both translations  
 and rotations of the body as a whole.

The equation of motion of the centre thus has the form

$$m\ddot{\mathbf{u}} = \frac{3}{2} c^2 \left( k_1 + \frac{1}{4} k_2 \right) \Delta \mathbf{u} + \frac{3}{4} c^2 k_2 \nabla \operatorname{div} \mathbf{u}. \quad (9)$$

Dividing this equation by the area  $\sqrt{3}c^2$  per particle in a  
 hexagonal lattice and introducing the two-dimensional  
 density  $\rho = m/\sqrt{3}c^2$ , we get

$$\rho \ddot{\mathbf{u}} = \frac{\sqrt{3}}{2} \left( k_1 + \frac{1}{4} k_2 \right) \Delta \mathbf{u} + \frac{\sqrt{3}}{4} k_2 \nabla \operatorname{div} \mathbf{u}. \quad (10)$$

Comparison of this equation with the macroscopic  
 equation of motion of an isotropic linear elastic continuum

$$\rho \ddot{\mathbf{u}} = \mu \Delta \mathbf{u} + (\lambda + \mu) \nabla \operatorname{div} \mathbf{u}, \quad (11)$$

gives for Lamé coefficients of the medium

$$\mu = \frac{\sqrt{3}}{2} \left( k_1 + \frac{1}{4} k_2 \right), \quad \lambda + \mu = \frac{\sqrt{3}}{4} k_2. \quad (12)$$

Thus, any isotropic elastic continuum, in the linear

approximation, can be described with the above lattice model.

### 3. Two-particle interaction potential

Interaction (2) depends only on the relative displacement of two selected neighbours and can thus be characterized as a “two-particle interaction”. To be able to describe large deformations, plasticity or rapture, as well as other effects where the particles leave their initial positions and may change the neighbours, one has to define a non-linear interaction, which depends not only on the initial but on the current neighbourhood. The simplest possible idea would be to define a two-particle interaction potential depending on a distance between particles only. However, it is impossible to define such a two-particle potential which has the linear expansion (2) and is compatible with the space symmetries. Indeed, a potential depending on the distance leads to central forces, which always have only projection onto the radius vector connecting the two particles. It can have only the second term in the expansion (2). The idea which we explore in this paper is the following: we define the interactions in such a way that they do depend explicitly on both the relative position of two particles and the orientation of the relative radius vectors with respect to the external lattice directions. At first glance, this coupling with the “external space” makes the system not invariant to the rotations of the medium as a whole. In reality, we have already shown that in linear approximation, the medium behaves as a normal isotropic continuum that is invariant with respect to the rotations. The whole non-symmetry is a surface effect. This is similar to the situation with the lattice gas [8], which simulates microscopically the isotropic fluid in spite of the underlying hexagonal symmetry of the lattice. The rotational symmetry in the linear range makes us sure that the particle system coupled with the hexagonal lattice directions can be used for realistic simulation of elastic and non-elastic behaviour of solids. In Section 4, we formulate a possible realization of such a “movable lattice particles” (MLP) model. The rest of the paper is devoted to investigation of its properties and simulation capabilities.

### 4. Model of MLPs

Effective dynamic equations of the model include a system of Langevin equations (which are Newtonian equations with the random noise source and dissipation term) completed by the “fictive forces” which return the vectors connecting interacting material points to (preliminary prescribed) symmetry axes.

In general case these equations for 2D-system can be written as follows:

$$\begin{aligned} \partial v_z / \partial t &= -\partial U / \partial z + F_{\text{return}}^z - F_{\text{diss}}^z + D\zeta, \\ \partial v_x / \partial t &= -\partial U / \partial x + F_{\text{return}}^x - F_{\text{diss}}^x + D\zeta. \end{aligned} \quad (12)$$

Here, the following notations are introduced:  $\partial x / \partial t = v_x$ ,  $\partial z / \partial t = v_z$ .

$$U = U(\mathbf{r}_j - \mathbf{r}_k) \quad (13)$$

is an arbitrary two-point potential which depends on the distance between the particles

$$r = ((x_j - x_k)^2 + (z_j - z_k)^2)^{1/2} \quad (14)$$

only and has an equilibrium minimum in a point  $r = r_0$ .

The dissipative force is proportional to the velocity:

$$F_{\text{diss}}^{x,z} \propto \eta v_{z,x}. \quad (15)$$

Random noise source as usually has the following correlators:

$$\begin{aligned} \langle \zeta(x, z; t) \rangle &= 0, \\ \langle \zeta(x, z; t) \zeta(x', z'; t') \rangle &= D \delta(x - x') \delta(z - z') \delta(t - t'). \end{aligned} \quad (16)$$

Here,  $\delta$  is the Dirac impulse function and intensity  $D$  is determined by the temperature of the system according to the fluctuation–dissipative theorem

$$D = 2k_B T \eta. \quad (17)$$

New terms are the “return functions”,  $F_{\text{return}}^{x,z}$ , which turn the vectors connecting each material point of the system with (nearest) neighbours, placed inside some proximity radius  $r_0$ , into a nearest symmetry axis. To define them we use a procedure which is illustrated in Fig. 1.

For each pair of the vectors  $\mathbf{r}_j$  and  $\mathbf{r}_k$ , a phase of the complex number

$$\varphi_{jk} = ((x_j - x_k) + i(z_j - z_k))$$

is calculated. After this, the projections are determined to fulfil the necessary rotation (which corresponds to a given rotation in the sector  $\{-\pi/6, \pi/6\}$  for the hexagonal six-fold symmetry or in the sector  $\{-\pi/4, \pi/4\}$  for the tetragonal four-fold symmetry). One has

$$\begin{aligned} F_{\text{return}}^x &= -f_0 \sin(\varphi) \sin(n\varphi), \\ F_{\text{return}}^z &= f_0 \cos(\varphi) \sin(n\varphi), \end{aligned} \quad (18)$$

where  $n = 4$  or  $n = 6$ , respectively.

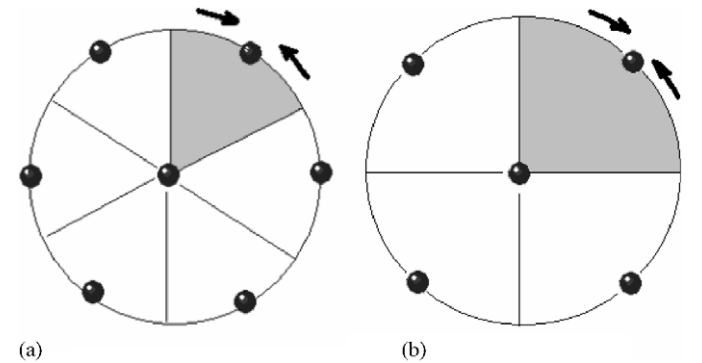


Fig. 1. Illustrations to the procedure which defines the additional forces for the hexagonal six-fold (a) and tetragonal four-fold (b) symmetries. Grey colour marks the sectors in which these forces tend to return the particles to particular symmetry axes ( $\pi/6$  or  $\pi/4$ , respectively).

1 The amplitude of the new force  $f_0$  is a new free parameter  
 3 which allows one to tune a value of the elastic modulus and  
 5 for the 2D-system hexagonal lattice with a fixed Poisson  
 ratio  $\nu = 1/3$ .

7 The same lattice takes place at nontrivial  $f_0$  and  $n = 6$ . It  
 9 differs only by the controlled value of the Poisson ratio. At  
 fixed other forces of the problem and a high enough value  
 11 into a square (tetragonal or, more generally, rhombic) one  
 at  $n = 4$ . In any case the symmetry of the lattice and its  
 13 elastic or even plastic properties have to be found a  
 posteriori, by performing numerical experiments which fix  
 15 a balance for different variants of the external loads.

## 5. Preliminary study of the MLP model

17  
 19 A crucial feature of the model is its ability to create and  
 21 keep under strong non-linear perturbations hexagonal and  
 tetragonal lattices prescribed by the additional forces  
 23  $F_{\text{return}}^{x,z}$ . To check this, we generate the lattice starting from  
 random initial conditions. The procedure was organized as  
 25 follows.

We put randomly placed particles inside a space region  
 27 which is (slightly) bigger than a region corresponding to the  
 ideal packing of the particles into a hexagonal or square  
 29 lattice. At fixed parameters of the potential  $U = U(\mathbf{r}_j - \mathbf{r}_k)$ ,  
 it has an equilibrium minimum at some  $r_0$  distance between  
 31 the particles, which determines a density of ideal structure.  
 At a low enough temperature  $U \gg T$ , the system tends to an  
 33 equilibrium which is close to such an ideal lattice with  
 appropriate symmetry.

35 It is important to stress that we do not apply here  
 periodic boundary conditions corresponding to the trans-  
 37 lation invariant system. Normally, such conditions force  
 some periodic arrangement of the particles, which is a  
 39 compromise between actual interactions of the system and  
 artificial periodicity of the boundary conditions. This  
 41 approach is natural for many other problems (e.g., in the  
 physics of phase transitions), but it is not the goal of this  
 43 study. Here, a structure, which appears in a course of the  
 relaxation, is allowed to be extremely imperfect. It can  
 45 include plenty of pores inside. But, it still has well-  
 pronounced local symmetry. Fig. 2 illustrates typical  
 47 results of such a procedure applied to four-fold and six-  
 fold symmetries (upper and down rows of plots, respec-  
 49 tively).

To control the results quantitatively, we apply a  
 51 standard approach of the solid-state theory. The Fourier  
 transform of the two-point correlation function is calcu-  
 53 lated according to the following procedure [9]:

$$55 \quad G(\mathbf{q}) = \int d^2\mathbf{r} G(\mathbf{r} - \mathbf{r}'), \quad (19)$$

57 where

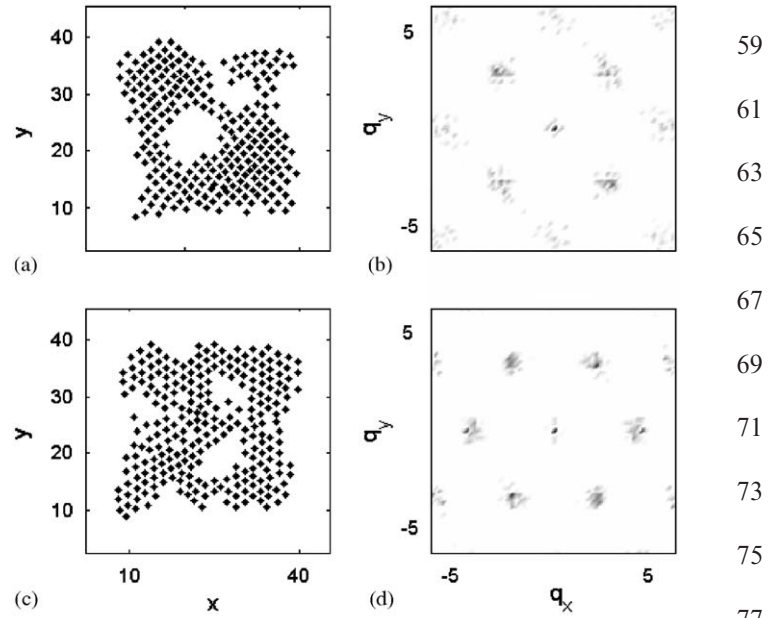


Fig. 2. Porous ordered structures generated from random initial conditions tetragonal and hexagonal symmetries accompanied by corresponding Fourier transforms of the two-point correlation functions ((a, b) and (c, d) subplots, respectively).

$$G(\mathbf{r} - \mathbf{r}') = \langle \rho_{\text{local}}(\mathbf{r}) \rho_{\text{local}}(\mathbf{r}') \rangle \quad (20)$$

and density of the discrete set of the particles is defined according to the usual receipt as a sum of the impulse Dirac functions

$$\rho_{\text{local}}(\mathbf{r}) = \sum_k \delta(\mathbf{r} - \mathbf{r}_k). \quad (21)$$

It is expected that for an ideal lattice, the Fourier transform has all correlation spheres (complete inverse lattice) of the maximums, but not a central group of the maximums only. It is seen from Fig. 2 that despite the small number of the particles  $N = 256$  (specially used for the illustration) and a strong imperfection of the porous structure, calculated correlation functions have well-pronounced symmetries. It means that one can take quite an arbitrary form of the “body” as an initial condition for any further numerical experiments.

One more challenge for the approach is to apply it to study the plastic deformations very far from an equilibrium. We performed a set of numerical experiments in this direction. It is found that at different intensities of an external load (as well as at different time dependences or geometries of the load), the system reproduces a wide variety of known dynamic scenarios. The “body” can oscillate elastically under a small load, or change its shape irreversibly, possessing plastic deformations, under higher loads. In the last case, the system goes via a number of quasi-static (metastable) equilibrium configurations into a final one and oscillates elastically around a new equilibrium.

To control the density evolution during the deformation process, we apply Gaussian convolution:

$$\rho(\mathbf{r}) = \sum_k \exp(-(\mathbf{r} - \mathbf{r}_k)^2/\lambda). \quad (22)$$

It is a widely used operation which allows one to find a density smoothed over short-time and scale fluctuations driven by the random noise. Fig. 3(a–f) presents principal stages of the plastic deformation. The density is shown by grey-scale map. White spots in the left subplots depict actual positions of the “particles” used to reconstruct the density by means of the convolution Eq. (22).

We start from the initial configuration of a rectangular slab with hexagonal internal symmetry (Fig. 3a). After an initial period of compressing caused by a strong enough external pressure (applied equally to the right and left boundaries of the slab), the system reaches a state of maximal density (Fig. 3c). A rate of plastic deformation at this stage reaches its maximum simultaneously. At later stages of the process, the system slowly goes to a new equilibrium which is shown in the subplot Fig. 3e. Right-hand-side subplots (Figs. 3b, d and f) present histograms of the density calculated for the above stages. It is seen

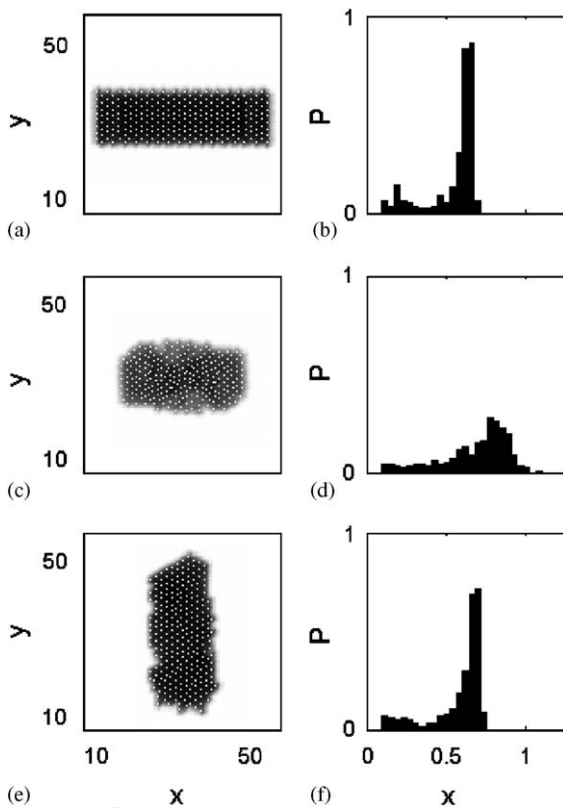


Fig. 3. Principal stages of the plastic deformation. White spots in the left subplots depict actual positions of the “particles” used to reconstruct the density by means of a Gaussian convolution described in main text. Initial configuration (a), a state of maximal density and rate of plastic deformation (c) and late stage of the process when system slowly goes to a new equilibrium (e) are shown. Right-hand-side subplots (b), (d) and (f) present histograms of the density calculated for these stages. The maximal rate of the plastic deformations corresponds to the state with maximal local densities (c) and maximal density fluctuations clearly seen in subplot (d).

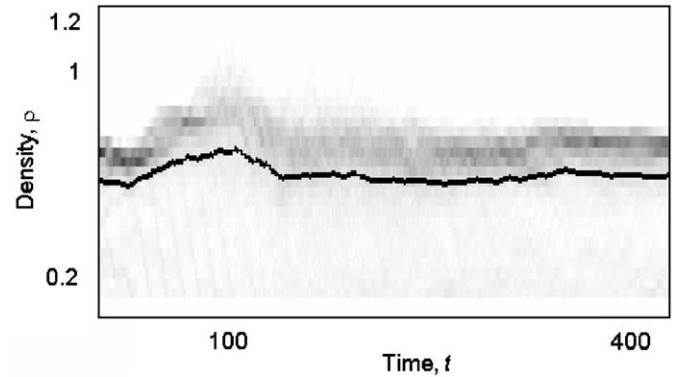


Fig. 4. Time evolution of the density distribution for the process presented in Fig. 3. Probability distribution is shown by the grey-scale map. Dark colour corresponds to high probability. Mean density for the whole system is plotted by the bold black line on the same scale. The region of maximum density coincides with its maximal standard deviations corresponding to a stage of fast plastic deformations shown by a pattern and histogram in Fig. 3(c) and (d), respectively.

directly from the subplot in Fig. 3d that the maximal rate of the plastic deformations at stage Fig. 3c) coincides with a period of maximal local densities and maximal density fluctuations.

A complete scenario of the process is seen in Fig. 4, which presents a time evolution of the density histograms by means of the grey-scale map. Dark colour corresponds to high probability. To compare this map with an evolution of the total density, we plot over the map a bold black line which depicts an evolution of the mean density on the same scale. This line lies below the dark grey regions due to an impact from the points which belong to a vicinity of the boundary. These points normally create a lower density which is seen as a flat light grey plateau down to the mean-density line.

To complete this preliminary study of the MLP model, we performed a calculation of the relative deformations under different external pressures. It is found that there is a critical pressure which separates elastic and plastic deformations. It is expected from a standard theory [10] to have a critical deformation amplitude (caused by a critical external force) which leads to the irreversible plastic deformation. So, it was an important test for the model to show that there is a pressure at which the “body” demonstrates such a transition. It starts with elastic deformation, goes to a critical elastic deformation and continues further with the plastic one.

To elucidate this, we calculate a relation between the maximal instant width of the body and the same value of trial specimen:

$$\delta h = [\max(y) - \min(y)] / \{[\max(y) - \min(y)]_{t=0}\}. \quad (23)$$

Fig. 5 presents three typical scenarios of the evolution. The black line in Fig. 5 corresponds to the elastic behaviour. Starting from zero deformation, the system quickly reaches an equilibrium (reversible) deformation

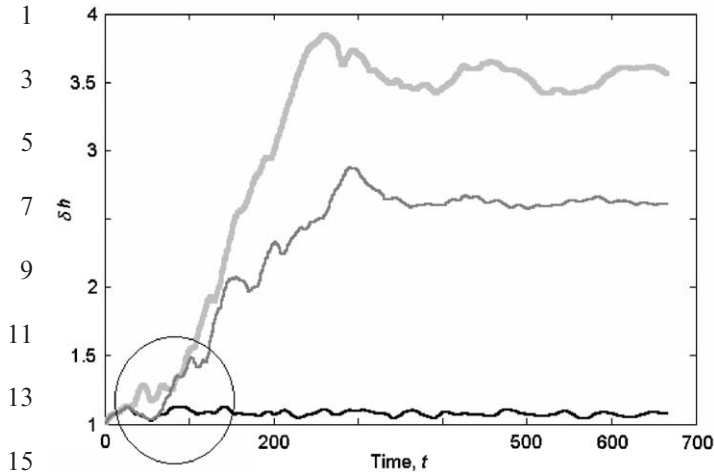


Fig. 5. Three typical scenarios of evolution of the maximal body width normalised to the same value of trial specimen. The black line corresponds to elastic behaviour; light grey curve corresponds to exactly the same plastic deformation as it is presented above in the Figs. 3 and 4. The circle marks a region where the separatrix (dark grey) curve follows the elastic line and joins the plastic curve.

and oscillates around it. A light grey curve presents the behaviour at high load. It corresponds to exactly the same plastic deformation as presented in the Figs. 3 and 4. The intermediate “separatrix” behaviour is shown by the dark grey curve. A thick circle marks the region where the separatrix follows to the elastic line and joins after to the plastic curve.

To test an applicability of the model to describe the friction processes, we studied the geometric configuration shown in Fig. 6. Two beams are brought in contact by a couple of pressing forces as in Fig. 3. At the same time, they are moved periodically by two (sinusoidal in time) transversal forces shown by grey arrows in the Fig. 6. A small enough pressure causes elastic distortions of the bodies, which do not affect their symmetry far from the contact region. But, friction of the bodies in the vicinity of the contact region strongly affects their structure. It produces strong deformations and randomizes structure. One can call this region as “liquid layer” between two rubbing bodies.

A natural way to describe quantitatively strong distortions of the structure in the frame of the model is to calculate a local absolute value of the “return functions”,  $F_{\text{return}}^{x,z}$ , which is mostly sensitive to the rearrangement:

$$\langle |F_{\text{return}}| \rangle = \langle [(F_{\text{return}}^z)^2 + (F_{\text{return}}^x)^2]^{1/2} \rangle. \quad (24)$$

The absolute value is taken here and average is performed over the  $y$ -direction

$$\langle \dots \rangle \equiv \int dy[\dots]/Ly \quad (25)$$

to extract regular information about return forces along the  $x$ -axis orthogonal to the contact surface. The lower subplot in Fig. 6 shows a relation between the mean value and different regions of the bodies. The correlation is seen

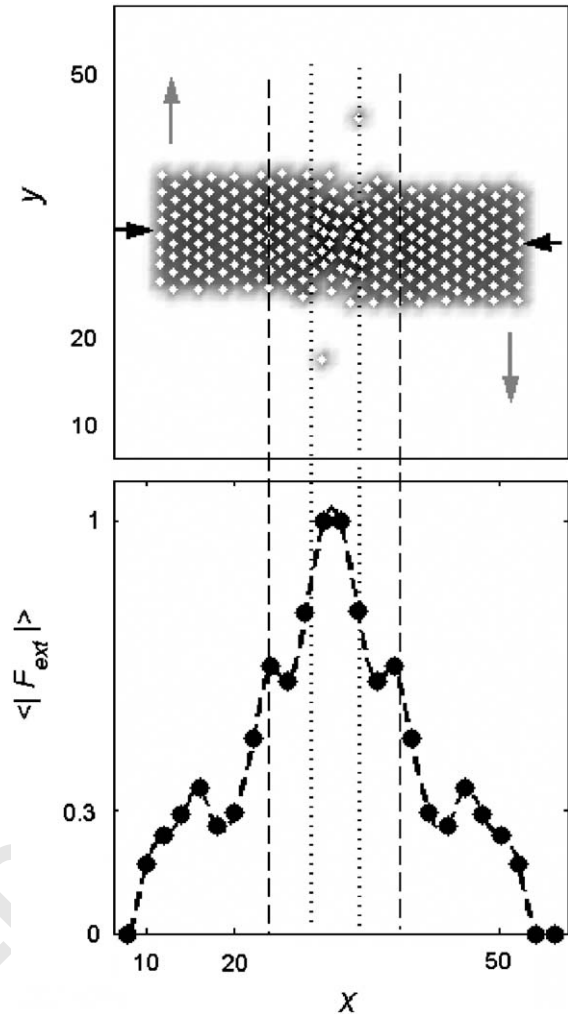


Fig. 6. Strong deformations in the vicinity of friction contact (“liquid layer”). The upper subplot shows instant configuration of the system. The lower subplot presents a correlation between the strong deformations in the contact vicinity and distribution of the mean return force,  $\langle |F_{\text{return}}| \rangle$ , averaged over the  $y$ -direction.

directly. In the closest vicinity of the contact, marked by the dotted lines, the value  $\langle |F_{\text{return}}| \rangle$  few times overcomes its value far from the region. There is also an intermediate region shown by dashed lines. In this region, the system still keeps its symmetry but the value  $\langle |F_{\text{return}}| \rangle$  is relatively high due to strong elastic deformation.

To conclude, it is shown that an approach, which combines a system of Langevin equations (Newtonian equations with the random noise source and dissipation term) and additional “fictive forces” returning the vectors connecting interacting material points to preliminary prescribed symmetry axes, allows one to describe a wide variety of realistic elastic and plastic systems.

#### Acknowledgement

The authors acknowledge financial support from the Deutsche Forschungsgemeinschaft.

1 **References**

- 3 [1] Greenspan D. Particle modelling in science and technology. Coll  
5 Math Societatis Janos Bolyai 1988;50:51.
- 7 [2] Ostermeyer GP. Many particle systems. In Proceedings of the  
9 German–Polish Workshop 1995. Warszawa: Polska Akad. Nauk,  
11 Inst. Podst. Prob. Techniki; 1996.
- 13 [3] Ostermeyer G-P. Mesoscopic particle method for description of  
thermomechanical and friction processes. Phys Mesomech  
1999;2(6):23–9.
- [4] Psakhie SG, Horie Y, Korostelev SYu, Smolin AYu, Dmitriev AI,  
Shilko EV, et al. Method of movable cellular automata as a tool for  
simulation within the framework of mesomechanics. Russ Phys J  
1995;38:1157–68.
- [5] Psakhie SG, Horie Y, Ostermeyer GP, Korostelev SYu, Smolin AYu,  
Shilko EV, et al. Movable cellular automata method for simulating  
materials with mesostructure. Theor Appl Frac Mech  
2001;37(1–3):311–34. 15
- [6] Popov VL, Psakhie SG. Theoretical foundations of simulation of  
elastoplastic media with the method of movable cellular automata. I.  
Homogeneous media. Phys Mesomech 2001;4(1):15–25. 17
- [7] Ostermeyer G-P, Popov VL. Solid–liquid transition described by the  
particle method. Tech Phys Lett 2000;26(3):250–3. 19
- [8] Frisch U, Hasslacher B, Pomenau Y. Lattice–gas automata for the  
Navier–Stokes equation. Phys Rev Lett 1986;56(14):1505. 21
- [9] Vakarin EV, Filippov AE, Badiali JP, Holovko MF. Phys Rev E  
1999;60:660. 23
- [10] Landau LD, Lifshitz EM. Theoretical physics, vol. V. Moscow:  
Nauka; 1965.

UNCORRECTED PROOF